

# L.U.N.A. - A Laser-Mapping Unidirectional Navigation Actuator

Jasper Zevering, Anton Bredenbeck, Fabian Arzberger, Dorit Borrmann and  
Andreas Nüchter

**Abstract** This paper proposes an autonomous approach to 3D mapping using the concept of conservation of angular momentum (COAM) as a unidirectional drive to roll a 2D laser scanner in an IMU equipped, pose-tracked spherical robot system. An experimental prototype of the robot is introduced, giving details about the hardware. The laser scanning results as well as the COAM drive data that have been gathered using the prototype are analyzed, revealing technical challenges.

## 1 Introduction

In today's world, autonomous robots have found their way into everyday life in a variety of ways. This includes, but is not limited to, the vacuum cleaner that independently navigates one's living-room or mobile robots employed for exploration of areas that are too dangerous for humans. To foster new advances in the latter, specifically for underground environments, the Defense Advanced Research Projects Agency (DARPA) of the US Defense Department established the yearly "SubT" Challenge in 2017. In this challenge, teams are tasked to "Drive novel approaches and technologies to allow warfighters and first-responders to rapidly map, navigate, and search dynamic underground environments." [4] proving the demand for further research in this domain. One subtask of this challenge is building an accurate 3D model of the environment, i.e., mapping the surroundings. This paper shows a proof of concept of a such a novel approach and validates it with experiments.

One such approach using a 2D laser scanner to scan 3D indoor environments has been proposed in [13]. The authors mount a 2D laser scanner on a cylindrical struc-

---

All authors are with Informatics VII – Robotics and Telematics, University of Würzburg, Am Hubland, 97074 Würzburg e-mail: [borrmann@informatik.uni-wuerzburg.de](mailto:borrmann@informatik.uni-wuerzburg.de)  
— e-mail: [jasper.zevering@stud-mail.uni-wuerzburg.de](mailto:jasper.zevering@stud-mail.uni-wuerzburg.de)  
— e-mail: [anton.bredenbeck@stud-mail.uni-wuerzburg.de](mailto:anton.bredenbeck@stud-mail.uni-wuerzburg.de)  
— e-mail: [fabian.arzberger@stud-mail.uni-wuerzburg.de](mailto:fabian.arzberger@stud-mail.uni-wuerzburg.de)

ture. An operator then initiates a rolling motion by manually pushing the contraption. This enables the scanner to sense the 3D environment successfully. However, manually pushing the scanner is not practical, especially for long scans.

Previous work includes our RADLER (RADial LasER scanning device), which consists of a 2D laser scanner attached to the axle of a unicycle [7]. An operator pushes the unicycle along a requested path. The inherent rotation of the wheel creates a radial 3D laser scanning pattern. However, this approach still requires an operator, therefore does not fulfill the autonomy requirements.

A more autonomous approach was taken by Fang et al. [9]. The authors mounted a rotating 2D laser-scanner on top of a turtle-bot thus removing the need of an operator. In contrast to the RADLER however, the turtle-bot does not provide an inherent rotation. Therefore an additional actuator is required to create the radial 3D scanning-pattern.

This paper builds upon the results of the RADLER and has a specific application of mapping lunar craters autonomously in mind. We propose a novel approach to low-cost 3D laser scanning using a 2D laser scanner inside a spherical robot based on conservation of angular momentum (COAM): the L.U.N.A. - sphere (Laser-mapping Unidirectional Navigation Actuator). The 2D laser scanner is fixed to the spherical structure, hence a similar situation as with the RADLER is given: the inherent rotation of the sphere creates a radial 3D scanning pattern. Using the format of a spherical robot permits the system to be designed more compact. Additionally, the spherical shell doubles as a protective layer for the actuators, sensors and electronics. This is especially valuable for applications in rough terrain or scenarios in which non-minimal impact is expected, such as space applications. During a launch, withstanding large G-forces is a necessary requirement, which can be better implemented using the spherical format. Furthermore, an operator is no longer required given a drive implemented in the robot.

## 2 State of the Art

As evolution of RADLER, a hand-driven radial scanner device, a self-driving spherical approach was chosen to ensure robustness and autonomy. The following presents different approaches to spherical robots.

An early idea of a self-driving sphere has been introduced by J.L. Tate in 1893 [16] for a sphere, driven by an inner moving counterweight, which got its torque from a spring. This idea of an actuator attached to a counterweight pointing to the bottom and therefore the torque being transferred to the sphere and moving it, is still a widespread approach for spherical robots.

In [8] a basic motion control system for the BYQ-III is introduced. The BYQ-III has a mass of 25 kg and a diameter of 600 mm and its driving mechanism has been proposed in [3] by Hanxu et al. It contains a counterweight pendulum, four gyro actuators, providing movement for two axes and one IMU mounted on the case of the gyro. There is no extra payload or sensor, nor would there be space for a centered

measurement unit due to the centered counterweight. Therefore the counterweight leads to a steady movement, not relying on acceleration but on velocity of the actuators and therefore providing continuous speed.

A second spherical robot with its driving mechanism relaying on inner counterweight is presented in [17]. This robot was designed for movement on a water surface and therefore has fins mounted to the shell orthogonal to the movement. Two actuators attached to the shell and the inner counterweight provide movement around one axis. In contrast to the BYQ-III a middle-centered sensor would be possible, but this would have no movement relative to the surface, as it would be part of the relatively non moving inner counterweight. It also has steady, well controllable movement. The spheres presented in [14] and [6] provide a solution for a driving system which does not rely on a moving inner counterweight but uses internal reaction wheels to provide torque. This leads to theoretically having middle-centered space available, which would be rotating with respect to the surface. However, the prototype provided by Muralidharan et al. [14] shows less controllability than counterweight driven spheres. Furthermore, this robot is driven by acceleration and not velocity which leads to limited movement capabilities.

A third approach for spherical robots relies on an internal unit which drives inside the sphere. A design and control approach is provided in [5] where a four-wheeled vehicle moves in the sphere to initiate rolling by moving the center of mass in the desired direction. This technical solution is capable of a nearly maximum size of possible payload in relation to the overall-size, but also does not provide a rotation of the sensor is needed for 3D laser scanning. Additionally, this provides good controllability, similar to the counterweight-driven approach. It is not stable regarding external perturbations or forces, as there is no fixed connection to the shell. This makes it not suitable for missions with extreme forces and unknown starting conditions like space applications involving a rocket launch or a hard landing to get to the starting point. In a worst case scenario this leads to a start with the unit being rotated by 180 degrees and therefore not being able to bring torque to the sphere. If the sphere is stuck a similar situation occurs. Then the inner unit tries to perform a whole revolution (“looping”) inside the sphere, which might result in a supine position.

Halme et al. [11] overcome this shortage of the inner unit with just relying on gravity to ensure contact to the shell. They introduce the approach of a rod, expanded by a spring to the maximum size and having a wheel on one side of the rod and the original unit on the opposite site. The wheel generates the motion by moving the center of mass, so the non-reversible supine position does not exist anymore. Even if the center of mass is at the top, the vehicle is still pressed to the shell by the spring and therefore is capable of maintaining its movement. This approach does not rotate a sensor placed in the center without further contraptions.

Inspired by the seminal Cubli [10], we started designing a spherical robot based on a conservation of momentum (COAM) drive.

### 3 Technical Approach

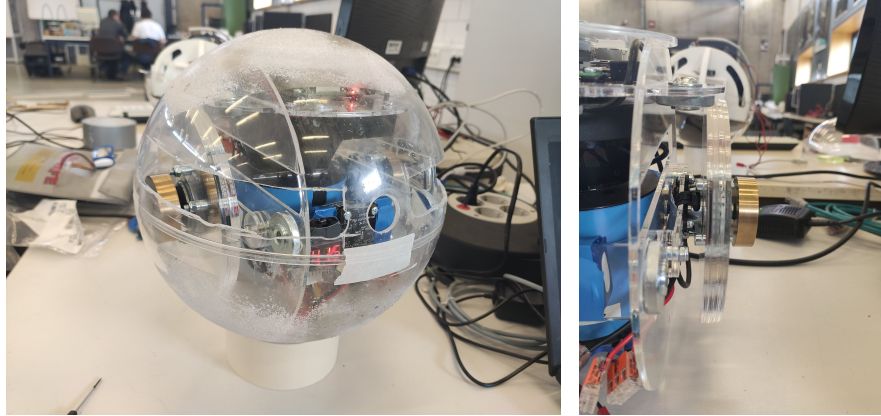


Fig. 1: Hardware setup of the L.U.N.A sphere prototype, including notches in the shell and friction granule (left). IMU (beneath supporting structure) and brushless motor including flywheel mass (above supporting structure) of the L.U.N.A sphere (right).

Wie dreht sich die Kugel überhaupt ? COAM + Cubli paper lesen / gyro effekt + video schneiden (ohne ton)

was ist da drinnen (raspberry pi, ..), wo ist es da drinnen, warum ist es da drinnen.

which is why measurement slits

Figure 1 shows the final hardware setup of the robot. In order to reduce complexity with respect to the 3D-transformation calculations, the laserscanner was placed at the center of a spherical acrylic glass shell as precisely as possible. This limits the laser scanners movement to rotational movement and removes translational movement completely. With this initial setup given, the only room left for the acrylic glass structural components, batteries, boardcomputer, IMUs, motors, weights and wiring are the spaces between the scanner and the shell. On each side one Turnigy Park480 brushless outrunner motor [2] of the COAM drive with two flywheels is attached. Strong epoxy glue attaches the weights to the motor shafts and shells. As the flywheels start spinning with respect to the structural components of the sphere, the sphere itself starts spinning with respect to the ground.

Figure 1 also shows that the top and the bottom of the shell are covered in table salt, which made a good granule to increase friction to the ground in the early testing phase. Furthermore, there are notches in the front side of the shell to increase permeability for the laser. Unfortunately, the laser scanner measurements are still affected by blockades due to components of the sphere. Specifically, the outside shell is an inhibiting factor as an object with the distance of the radius is measured at all times.

Figure 2 shows a CAD blueprint of the overall interior layout of the mechanical structure of the L.U.N.A sphere, ignoring the outside sphere, flywheels and wiring. The payload is mounted to supporting structural components which are made of

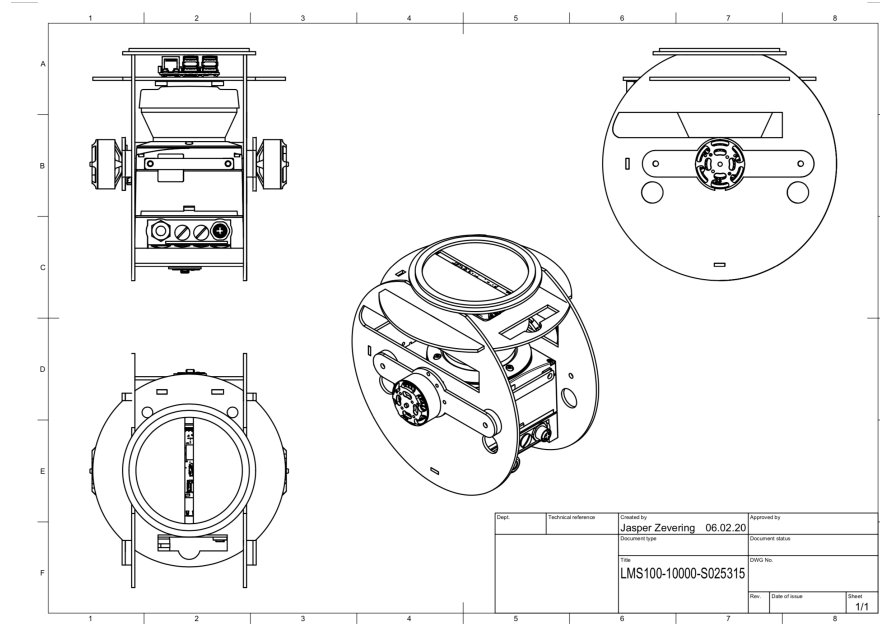


Fig. 2: Blueprint of the mechanical structure of the spherical robot.

acrylic glass. The Raspberry Pi 3B boardcomputer is placed on top of the laser. Above that, another supporting structure holds additional counterweights to correct for inhomogeneous weight distribution. The battery finds its place in front of the laser scanner on another supporting structure. The two brushless motors were each placed on one side of the supporting structure with spacers that leave room for the side IMU underneath one of the motors. Two other IMUs are placed in front of and beneath the laser to ensure coverage of all axes.

### 3.1 Sensor Integration

The sensor integration is fully implemented with the Robot Operating System (ROS) using the Ubuntu distribution [ROSberryPi](#) which contains a pre-installed ROS version. Overall, three separate PhidgetsSpacial 10441B IMUs [1] keep track of the pose of the sphere. Each IMU is placed in such a way that the IMUs Z-axis corresponds to one possible rotation axis of the sphere. Therefore, each IMU is perpendicular to the other two. Combining the axes measurements leads to a "virtual" IMU, which emulates being an IMU positioned at the center of the sphere. Hence, isolating the measurements of the resulting virtual IMU to only the rotation in the given axis. Figure 3 illustrates this principal. Previous prototypes have shown that

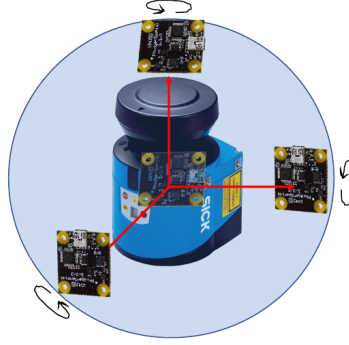


Fig. 3: Sketch that helps illustrate the combination of 3 IMUs into 1 virtual IMU that simulates being at the center of the sphere.

transforming the data of only one non-centered IMU leads to lower quality measurements. However, combining the measurements of three IMUs, where each measures only the static rotation around one of their rotational axes (which also represents a rotation axis of the sphere), leads to less noise, as seen in figures 4a-4d.

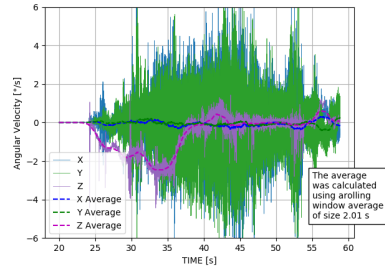
The IMUs also ship with accelerometers that are used to determine the full pose of the sphere. Each IMU calculates their pose separately, using a quaternion extended Kalman filter (QEKF). However, combining those poses into one does not have any positive effect, but only makes the software more resource demanding and slow. Thus only the pose of the bottom IMU's accelerometer is used to keep track of the pose.

The motors are controlled using the piGPIO library. The GPIO signals are forwarded by the pins to two ESCs that drive the motors.

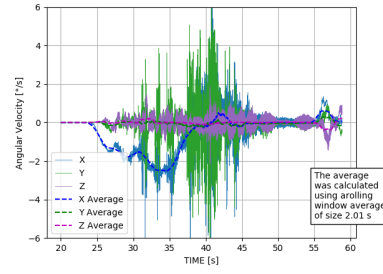
Unfortunately, the brass weights are not drilled in the very center, causing an unbalance when rotating. The resulting vibrations inhibit the movement of the sphere. Thus a controller was implemented that measures the extend of the vibrations using standard deviations of the non-rotating axes of the IMU and adjusts the throttle of the motors accordingly. This was done with a two-point controller with hysteresis. Considering the translational velocity of the sphere in a controller is not possible. The speed of the sphere is calculated by the rotational speed, which is why slippage of the sphere causes such a controller not to produce the desired motion.

### 3.2 Point Cloud Processing

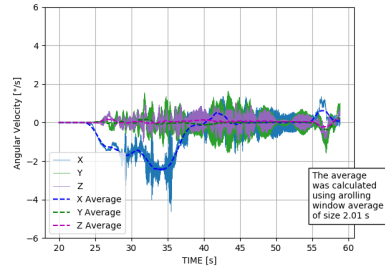
For the processing of the point cloud the 3D Toolkit (3DTK) was used. This provides multiple methods and algorithms for processing 3D point clouds, especially the 6D continuous time Simultaneous Localization And Mapping (SLAM) algorithm (see [15, 12]) as post-processing. Therefore only the time-stamped raw data of the IMUs



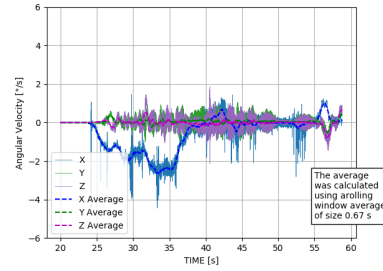
(a) IMU 1: Z-Axis corresponds to Sphere X-Axis



(b) IMU 2: Z-Axis corresponds to Sphere Z-Axis



(c) IMU 3: Z-Axis corresponds to Sphere Y-Axis



(d) Merged virtual IMU. Maps the Z-Axis of all other IMUs to the rotational axes.

Fig. 4: Angular velocity measurements of singular IMUs and the combined IMU.

and laser-scanner is transferred and the estimation of the pose and the SLAM algorithm itself is performed externally. For this prototype the transfer is realized using the host-function of ROS, giving the external PC the possibility to subscribe to the topics and process them. 3DTK itself takes pairs of files, one representing the pose, one the laser scanner data, and each file named by the time-stamp with an identifier if it is scan-data or pose. Also, the use of USB-connected IMUs and ROS as transfer-mechanism of data leaves potential for enhancement and therefore reducing the load of the internal controller.

## 4 Experimental Results

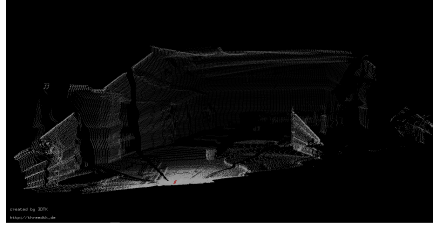
### 4.1 3D Laser Scanning

The test of the 3D laser scanning consists of 3 phases. First a semi stationary scan is performed by moving the robot manually in a limited manner (tilting it by approx-

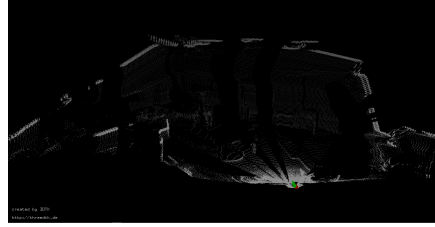


imately  $45^\circ$ ) without its exterior shell. This results in the 3D point cloud in figure 5a. For the second test the same movement is used. However, this time the outside shell of the robot is present. This results in figure 5b. Finally, the COAM-drive enabled test of the overall system leads to a 3D point cloud consisting of multiple revolutions. Figure 5c shows results.

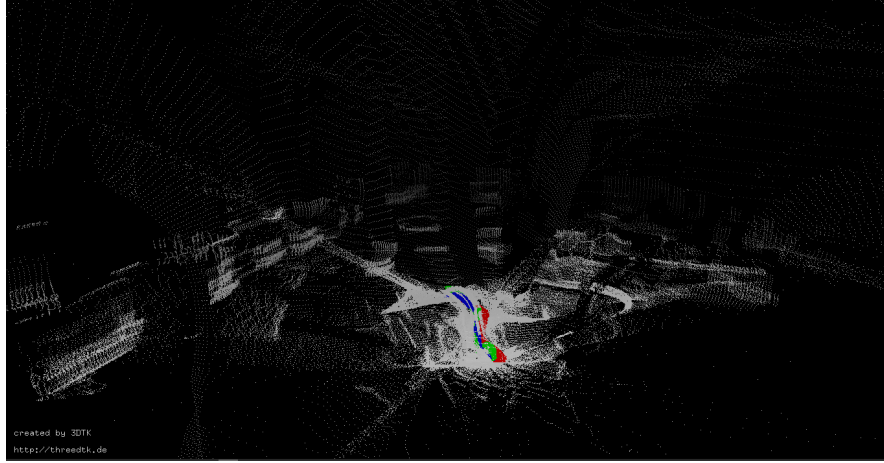
Point size increase,  
maybe black on  
white?



(a) Test with limited movement and no exterior shell.



(b) Test with limited movement but present exterior shell.



(c) Test with exterior shell and full movement (i.e. multiple revolutions).

Fig. 5: 3D Point cloud results of different test scenarios of the system.

The first test yields the clearest 3D point cloud (figure 5a). This is contributed to the fact, that in this test the exterior shell is absent. Since the shell partially reflects the beams of the laser scanner, the noise level increases. In this case the laser scanner measures the shell instead of the environment around it. In figure 5b lines are blocked that are measured in the previous test further showing the reflection of the laser beams by the shell. The rolling motion of the robot increases this effect. Specifically, a large number of measurement points along the path of the robot manifests this (figure 5c). We assume that the more powerful laser scanner LMS141 reduces this effect.



Furthermore, the time asynchrony of the pose determination sub-system and the laser scanner introduces further systematic errors to the 3D point cloud. Specifically, figure 5c shows that the laser scanner detects points underneath the surface the robot was rolling on.

## 4.2 COAM Drive

The conversation of angular momentum drive accelerates the L.U.N.A. sphere reliably. Figure 4 shows the angular acceleration of the whole sphere measured by the IMU system in one test run. Furthermore, it shows that the acceleration along the rotational axis of the flywheels rises while the accelerations along the other axes remain lower, albeit are noisy. However, it also shows the decrease in noise due to the combination of the IMU measurements. The vibrations and tilt of the robot contribute to the velocities along the other axes. The vibrations are results of inexact drilling of the flywheels such that there is an unbalance. At the main test site the ground is a hard, clean and low friction concrete floor. In such a scenario the vibrations add up and lead to slippage. However, a rubber surface (a running track) absorb the vibrations, such that the acceleration process happens reliably.

## 5 Conclusions

This paper has presented a new cost efficient approach to 3D laser scanning: The L.U.N.A. sphere. It uses a 2D laser scanner mounted inside a spherical robot and the inherent rotational movement to form a radial scanning pattern, hence creating a 3D point cloud. The spherical robot is based on conversation of angular momentum and uses flywheels to drive the robot forward.

The prototype developed for the tests in this paper was able to move in one direction reliably on soft surfaces (such as rubber), however had difficulties with slippage on hard and low friction surfaces.

With regards to 3D laser scanning this paper has delivered a proof of concept, even though the results leave room for improvement. Needless to say, a lot of work still has to be done. In future work, we plan to overcome the biggest issues, i.e, the reflection of the laser beams by the exterior shell and synchronization issues between the IMU system and the laser scanner.

This includes improving the field of view of the laser scanner and extending the robot to two dimensional movement control. This enables autonomous mapping of environments using the L.U.N.A. sphere.

## Authors Note

In an attempt to abide by the [Fair-Principles](#) of open science the authors provided all code developed and further information at their [GitHub](#) page.

**Acknowledgements** The authors thank Dieter Ziegler and Sergio Montenegro for supporting our work and the Elite Network Bavaria for providing funding.

## References

1. Phidgets imu website. <https://www.phidgets.com>. Accessed: 2020-04-15.
2. Turnigy park480 brushless outrunner. [https://hobbyking.com/en\\_us/turnigy-park480-brushless-outrunner-1320kv.html](https://hobbyking.com/en_us/turnigy-park480-brushless-outrunner-1320kv.html). Accessed: 2020-04-17.
3. Omnidirectional kinematics analysis on bi-driver spherical robot. In *Journal of Beijing University of Aeronautics and Astronautics* 31, pages 735–739, July 2005.
4. Booz Allen. Unearthing the subterranean environment. <https://www.subtchallenge.com>. Accessed: 2020-04-06.
5. J Alves and J Dias. Design and control of a spherical mobile robot. *Proceedings of the Institution of Mechanical Engineers, Part I: Journal of Systems and Control Engineering*, 217(6):457–467, 2003.
6. S. Bhattacharya and S. K. Agrawal. Spherical rolling robot: a design and motion planning studies. *IEEE Transactions on Robotics and Automation*, 16(6):835–839, 2000.
7. D. Borrmann, S. Jörissen, and A. Nüchter. RADLER - A RADial LasER scanning device. In *Proceedings of the 16th International Symposium of Experimental Robotics (ISER '18)*, Springer Tracts in Advanced Robotics, pages 655–664, Buenos Aires, Argentina, November 2018.
8. Daliang Liu, Hanxv Sun, Qingxuan Jia, and Liangqing Wang. Motion control of a spherical mobile robot by feedback linearization. In *2008 7th World Congress on Intelligent Control and Automation*, pages 965–970, 2008.
9. Zheng Fang, Shibo Zhao, Shiguang Wen, and Yu Zhang. A real-time 3d perception and reconstruction system based on a 2d laser scanner. *Journal of Sensors*, 2018:1–14, 05 2018.
10. M. Gajamohan, M. Merz, I. Thommen, and R. D’Andrea. The cubli: A cube that can jump up and balance. In *International Conference on Intelligent Robots and Systems*, pages 3722–3727, 2012.
11. Aarne Halme, Jussi Suomela, Torsten Schönberg, and Yan Wang. A spherical mobile micro-robot for scientific applications. *ASTRA*, 96, 1996.
12. H. A. Lauterbach, D. Borrmann, A. Nüchter, A. P. Rossi, V. Unnithan, P. Torrese, and R. Pozzobon. Mobile mapping of the la corona lavatube on lanzarote. In *Proceedings of the ISPRS Geospatial Week 2019, Laserscanning 2019*, ISPRS Annals Photogrammetry and Remote Sensing, Spatial Inf. Sci., IV-2/W5, pages 381–387, Enschede, Netherlands, June 2019.
13. Ville Lehtola, Juho-Pekka Virtanen, Antero Kukko, Harri Kaartinen, and Hannu Hyypp. Localization of mobile laser scanner using classical mechanics. *ISPRS Journal of Photogrammetry and Remote Sensing*, 99:25 – 29, 01 2015.
14. V. Muralidharan and A. D. Mahindrakar. Geometric controllability and stabilization of spherical robot dynamics. *IEEE Transactions on Automatic Control*, 60(10):2762–2767, 2015.
15. A. Nüchter, M. Bleier, J. Schauer, and P. Janotta. Improving Google’s Cartographer 3D Mapping by Continuous-Time SLAM. In *Proceedings of the 7th ISPRS International Workshop 3D-ARCH 2017: "3D Virtual Reconstruction and Visualization of Complex Architectures"*,

- ISPRS Archives Photogrammetry and Remote Sensing Spatial Inf. Sci., Volume XLII/W3, pages 543–549, Nafplio, Greece, March 2017.
16. J.L. Tate. Method and system for measurement of road profile, 14 1893. US Patent 508,558.
  17. H. Vahid Alizadeh and M. J. Mahjoob. Quadratic damping model for a spherical mobile robot moving on the free surface of the water. In *2011 IEEE International Symposium on Robotic and Sensors Environments (ROSE)*, pages 125–130, 2011.